Received: January 6, 2025 | Revised: March 17, 2025 | Accepted: March 25, 2025

JOURNAL OF APPLIED RESEARCH ON SCIENCE AND TECHNOLOGY
INSTITUTE OF RESEARCH AND DEVELOPMENT
RAJAMANGALA UNIVERSITY OF TECHNOLOGY THANYABURI
JARST
ISSN ONLINE: 2773-9473
https://ph01.tci-thaijo.org/index.php/rmutt-journal

Fabrication of uric acid chemical sensor based on tricobalt tetroxide crosslinked chitosan with gold nanoparticle modified glassy carbon electrode

Nuenghathai Chaiya[1], Suphaporn Chenkhuruthum[1], Ratchadaporn Puntharod[2], Anchana Preechaworapun[3], Pusit Pookmanee[2] and Tanin Tangkuarum[2*]

[1]Applied Chemistry Program, Faculty of Science, Maejo University, Chiang Mai, THAILAND

[2]Chemistry Program, Faculty of Science, Maejo University, Chiang Mai, THAILAND

[3]Department of Chemistry, Faculty of Science and Technology, Pibulsongkram Rajabhat University, Phitsanulok, THAILAND

[*]Corresponding author: tanin.tang@gmail.com

ABSTRACT

Sensor technology has advanced significantly in recent years and has become an essential tool in various fields, including medicine, food analysis, and environmental monitoring. Uric acid (UA) is a biomarker for several diseases, such as gout and kidney stones. This research develops an electrochemical sensor for the determination of UA based on tricobalt tetroxide (Co_3O_4) and gold nanoparticles (AuNPs) in the crosslinked chitosan polymer (CHIT) and modified on the glassy carbon electrode (GCE) (Co_3O_4-CHIT/AuNPs/GCE). X-ray diffractometer (XRD) and scanning electron microscope (SEM) were used to characterize the synthesized Co_3O_4, which was crystallized in a cubic phase with a flower-like structure, while AuNPs were successfully synthesized and confirmed by UV-Vis spectroscopy. The Co_3O_4-CHIT/AuNPs/GCE was tested in 0.15 mM of UA using cyclic voltammetry (CV) and gave an oxidation peak at +0.61 V. The Co_3O_4-CHIT/AuNPs deposited on GCE exhibited the ability to oxidize the UA and obtained a higher current compared to the bare, Co_3O_4-CHIT, and AuNPs modified electrodes for 1.79, 2.03, and 1.47 times, respectively. The analytical specification of this sensor was studied by amperometric technique in phosphate buffer pH 7.0 at suitable parameters of applied voltage, AuNPs, and Co_3O_4-CHIT for + 0.65 V, 20 µL, and 60 µg, respectively. It was found that the linearity obtained from 0.5 to 700 µM ($y = 0.0079x + 0.0049$, $R^2 = 0.9996$) with a limit of detection (LOD) of 0.31 µM (S/N =3) and limit of quantification (LOQ) was calculated to be 1.03 µM. We found that 0.01 mM ascorbic acid, 0.5 mM urea, 0.1 mM caffeine, 5.0 mM Cl^-, 7.0 mM glucose, and 20.0 mM sucrose did not affect the UA analysis. The repeatability and reproducibility were obtained at 2.94 %RSD (n=5) and 2.30 %RSD (n=5), respectively. This sensor was applied to detect uric acid in blood samples without any preparation before the test. It showed high accuracy in terms of %recovery within the range of 96.76-104.92.

Keywords: Glassy carbon electrode, Tricobalt tetroxide, Chitosan crosslinking gold nanoparticle, Uric acid

INTRODUCTION

Uric acid (UA) is a waste product produced when the body breaks down purines, which are found in many foods such as red meat, poultry, seafood, drinks with high fructose corn syrup, and alcohol. It is created from processed chemical purines in the body for repair or building cells. UA in human metabolism is excreted via urine by the kidneys. It is recommended that the blood level of men should not exceed 7 mg/dL and that of women, not over 6 mg/dL [1]. However, some references showed that the recommended range of UA in blood for adult males is 4.0-8.5 mg/dL or 0.24-0.51 mM; for adult females, it is 2.7-7.3 mg/dL or 0.16-0.43 mM. UA levels play a crucial role in maintaining health. Elevated UA levels are associated with conditions such as gout, kidney stones, renal failure, and kidney disease. Conversely, lower UA levels have been linked to neurological disorders, including multiple sclerosis, Parkinson's disease, Alzheimer's disease, Fanconi syndrome, and optic neuritis. However, due to UA's antioxidant properties, it contributes to brain protection [2]. Currently, UA levels in the blood are detectable via a variety of medical diagnostic tests, such as high-performance liquid chromatography (HPLC) [3, 4] and spectroscopy [5]. However, these techniques are time-consuming and require specialized equipment and trained personnel. As a result, there is growing interest in the development of methods for UA that can be used for rapid and accurate monitoring of the blood or other bodily fluids using a variety of techniques, such as electrochemical [6-8], optical [9], and colorimetric [10] methods.

DOI: 10.60101/jarst.2024.260199

The electrochemical method is more popular than other techniques as it possesses rapid analysis times, simple experimental procedures, and inexpensive instrumentation. Different electrochemical techniques have been applied for the detection of target analytes, including cyclic voltammetry (CV) [11, 12], electrochemical impedance spectroscopy (EIS) [13], and differential pulse voltammetry (DPV) [14, 15]. Omar et al. [16] have reported the immobilization of uricase onto graphene oxide (GO) and using 1-ethyl-3-(dimethylaminopropyl) carbodiimide (EDC) and N-hydroxysulfosuccinimide (NHS) as crosslinking reagents on glassy carbon electrode (GCE) for the detection of uric acid (UA) via cyclic voltammetry (CV). They found a linear dependence on the UA concentration ranging from 0.02 to 0.49 mM with a detection limit of 3.45 mM and presented good reproducibility. Jirakunakorn et al. [17] developed a method by immobilizing uricase on a porous cryogel platform of graphene-incorporated chitosan (CHIT) on top of a Prussian blue layer (PB) by electrodeposition on a screen-printed carbon electrode (SPCE). They employed an amperometric detector integrated with a flow-injection system, which showed a linear detection range from 0.0025 to 0.40 mmol L^{-1} and a detection limit of 2.5 µmol L^{-1}. Remarkably, common interferents in human serum samples had no significant effect on the detection performance. These reports show the advantages of electrochemical sensors.

Tricobalt tetroxide (Co_3O_4) is still used in various industries and research. It has oxidation numbers of 2+ and 3+ and crystallizes in a cubic structure [18]. Its properties are high surface area, good conductivity [19], strong catalytic activity, and p-type semiconductor [20], These properties make it an ideal material for use in sensors [21, 22], supercapacitors [23], and catalytic [24]. Gold nanoparticles (AuNPs) have a high surface area-to-volume ratio [25] and possess good biocompatibility [26]. It continues to be popular and is still used with various syntheses, such as green synthesis [27]. Numerous studies have explored the applications of AuNPs, such as Ismail et al. [28], the development of an electrochemical sensor based on silica/gold nanoparticles for the detection of arsenic, and Qingshan Yang et al. [29], the development of a glucose sensor using AuNPs and glucose-oxidase. Chitosan (CHIT) is classified as a natural biopolymer, with properties that enable gelling and membrane formation [30]. In the last few years, its applications have expanded to include medicine for wound healing, drug delivery, and tissue engineering due to its biocompatibility and antimicrobial activity. Moreover, they obtained interest from electrochemical sensors for immobilizing nanomaterials, increasing the sensitivity, selectivity, and stability of the electrochemical sensors [31]. For example, CHIT was utilized in improving the stability of glucose sensors based on hydrogels [32], and Chachuli et al. present a polymer-based gas sensor comprising chitosan as binder and graphene as a sensing material for acetone and ethanol [33].

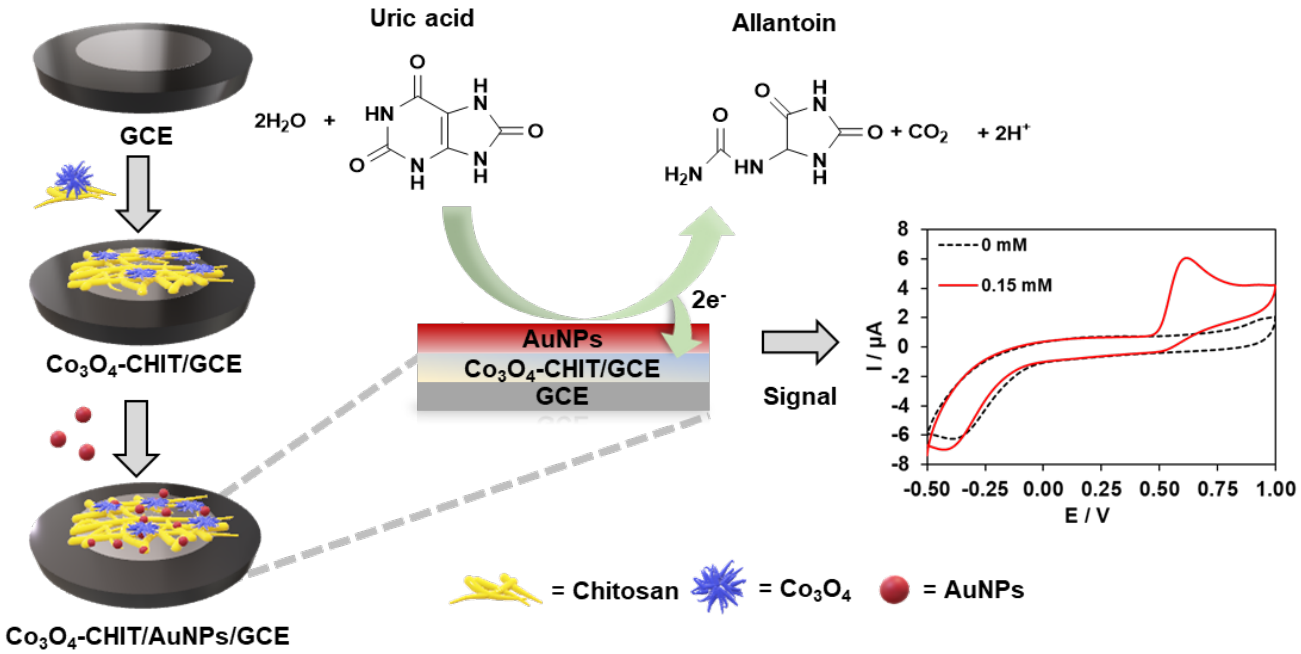

Scheme 1 The fabrication process of the sensor and possible mechanism for UA detection.

Based on our knowledge, there is no report of the fabrication of Co_3O_4 with biocompatible polymers such as CHIT and AuNPs. This research aims to synthesize Co_3O_4 with AuNPs in CHIT polymer to determine UA in blood samples by an electrochemical technique. Hence, this work presents a significant challenge due to the absence of enzymes for UA detection. The primary advantage of this approach is the enhanced long-term stability of the electrodes, as enzymes typically limit the sensor's lifespan and are highly sensitive to temperature fluctuations and chemical interference. Furthermore, eliminating the need for enzymes

DOI: 10.60101/jarst.2024.260199

JOURNAL OF APPLIED RESEARCH ON SCIENCE AND TECHNOLOGY

contributes to cost reduction. Scheme 1 showed the fabrication and conceptual model of possible mechanisms for detecting UA. It was oxidized into allantoin, releasing two electrons and two protons [6, 34]. The obtained current was facilitated by Co_3O_4-CHIT/AuNPs and measured by an electrochemical technique of cyclic voltammetry and amperometry.

MATERIALS AND METHODS

Materials

The cobalt nitrate hexahydrate (99%), and glacial acetic acid were obtained from QRëC (New Zealand). Caffeine (99%), disodium hydrogen phosphate (99%), L-ascorbic acid (99.5%), sodium borohydride (97%), sodium acetate (99.5%), and sodium chloride (99.5%) were provided by Loba Chemie Pvt. Ltd. (India). The D-glucose (99.5%) anhydrous was provided by Ajax Finechem (NSW, Australia). Urea (99%), sodium hydroxide (97%), and potassium dihydrogen phosphate (99.5%) were supplied from RCI Labscan (Bangkok, Thailand). Chitosan (low molecular weight, 75%), uric acid (UA, 99%), gold (III) chloride trihydrate (49%), sodium citrate tribasic dihydrate (99%), and sucrose (99.5%) were received from Sigma-Aldrich, USA. Glutaraldehyde solution (~50%) was provided by Fluka, USA.

All measurements of voltammetry and amperometry were operated with CH1230A (CH instrument, USA) which was controlled by a personal computer. A conventional three-electrode system equipped with a bare glassy carbon electrode (GCE) or the modified GCE as working electrodes, (CH instrument, Ø 3 mm), a Pt wire electrode (CH instrument, Ø 0.5 mm and 3.2 cm long) as a counter electrode, and an Ag/AgCl (3.0 M KCl internal solution, CH instrument) as a reference electrode. All solutions used in this study were prepared with 18.2 MΩ-cm ultrapure water (ZMQ50007, Milli-Q Academic, USA).

Synthesis of gold nanoparticles (AuNPs)

The AuNPs synthesis procedure was adapted from our previous reports[35]. Briefly, 0.01% w/v gold (III) chloride trihydrate, 10 mM sodium borohydride, and 10.0 mM sodium citrate were mixed in a beaker at the mole ratio of Au:$Na_3C_6H_5O_7$:$NaBH_4$ by various 1:0:19, 1:2:17, 1:4:15, 1:9:10, 1:14:5, 1:17:2, and 1:19:0respectively, and vigorously stirred by magnetic stirrer for 15 minutes. Then, the solution was transferred to a hydrothermal synthesis reactor and heated at 120 °C for 30 minutes to obtain AuNPs solution. AuNPs were characterized via scanning absorption spectrum mode by UV-vis spectroscopy (UH5300, Hitachi, Japan).

Synthesis of tricobalt tetroxide (Co_3O_4)

Co_3O_4 was synthesized by modifying the method of Ramesh Lal et al. [36]. Briefly, 0.01 M cobalt nitrate and 0.01 M urea were dissolved in 80 mL of deionized (DI) water in a beaker and stirred for 15 minutes. Next, the solution was transferred to a hydrothermal reactor and heated at 95 °C for 6 h. Then, the suspension in the reactor was evaporated at 80 °C in the hot air oven. Finally, the precipitate was calcined at 500 °C for 5 hours to get tricobalt tetroxide in black-color powder. This synthesized material was characterized by an X-ray diffractometer (XRD) (Bruker, D8, Germany) and scanning electron microscope (SEM) (VEGA, TESCAN, Czech Republic).

Preparation of modified electrode

Co_3O_4-CHIT/AuNPs were deposited on the GCE as follows. Co_3O_4 3.0 mg was dispersed in 1.0 mL of 0.5% CHIT-crosslinked glutaraldehyde by ultrasonicated for 30 min. CHIT acts as a binder to immobilize Co_3O_4 on the electrode surface to ensure strong adhesion and stability of the modified layer. The GCE was cleaned by polishing with a slurry of 0.05 µm Al_2O_3 and rinsed thoroughly with UW. An aliquot of 20.0 µL of Co_3O_4-CHIT was dropped on the cleaned bare glassy carbon electrode surface and left to dry at room temperature. In the last step, 20.0 µL AuNPs solution was placed and left to dry. The Co_3O_4-CHIT/AuNPs/GCE modified electrode was obtained and rinsed with UW before use. AuNPs/GCE and Co_3O_4-CHIT/GCE modified electrodes were modified similarly to Co_3O_4-CHIT/AuNPs/GCE.

Samples analysis

Real blood samples were donated from Sansai Hospital, Sansai district, Chiang Mai, Thailand. The samples were determined for UA without any preparation by the standard addition method.

RESULTS AND DISCUSSION

Characterization of materials

XRD and SEM techniques revealed the crystal phase and morphology of the synthesized Co_3O_4. The XRD pattern of Co_3O_4, as shown in Figure 1A, exhibits diffraction peaks at (111), (220), (311), (222), (400), (422), (511), (440), and (533), which correspond to the cubic crystal structure according to the JCPDS 00-011-1152 reference. Figure 1B shows an SEM image of Co_3O_4 flower-like. The gold nanoparticle (AuNPs) solutions exhibited different colors depending on the molar ratio of Au:$Na_3C_6H_5O_7$:$NaBH_4$ as in Figure 1C. This phenomenon is attributed to the size-dependent optical properties of AuNPs [37]. To confirm the identity of the synthesized AuNPs, their absorbance was measured using a UV-visible spectrophotometer. The absorption spectra were recorded in the 250-800 nm wavelength range. The results indicated that the synthesized AuNPs solutions exhibited maximum absorbance in the range of 520–530 nm as shown in Figure 1D. Surface plasmon resonance (SPR) wavelength is primarily influenced by particle sizes [38]. In the

DOI: 10.60101/jarst.2024.260199

sample with a molar ratio of 1:17:2, the SPR peak appeared at 520 nm with the highest absorbance (0.247), indicating that this sample had the smallest particle size, and the highest concentration compared to other ratios. Due to these favorable characteristics, this AuNPs was selected for further experiments.

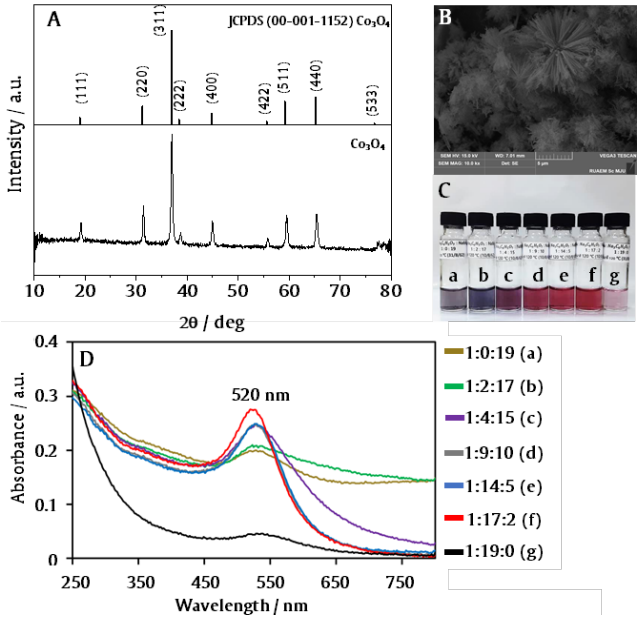

Figure 1 (A) XRD pattern (B) SEM image of Co_3O_4. (C) Photograph and (D) UV-vis spectra of AuNPs solutions at different mole ratios of Au:$Na_3C_6H_5O_7$:$NaBH_4$ at 1:0:1 to 1:19:0 for a to g, respectively. The Labels (a-g) in C and the legends (a-g) in D show the correspondence between C and D.

Cyclic voltammetry of UA

The cyclic voltammogram of 0.15 mM UA was measured in 0.1 M PBS (pH 7.0) at modified/unmodified GCE electrodes to study the electrochemical behavior of UA in Figure 2. The oxidation peak of UA at bare (Figure 2-black), Co_3O_4-CHIT/GCE (Figure 2-brown), AuNPs/GCE (Figure 2-blue), and Co_3O_4-CHIT/AuNPs/GCE (Figure 2-red) appeared at +0.58 V, +0.60 V, +0.60 V, and +0.61 V, respectively. The absence of a reduction peak confirms that the oxidation of UA is an irreversible process in solution. During oxidation, UA donates two electrons and two hydrogen ions, forming allantoin as the primary oxidation product [34, 39]. The reaction mechanism can be represented as reaction (1):

$$\text{Uric acid} + 2H_2O \rightarrow \text{Allantoin} + CO_2 + 2e^- + 2H^+ \quad (1)$$

While oxidation currents were found for 2.94 µA, 2.58 µA, 3.57 µA, and 5.25 µA for bare, Co_3O_4-CHIT/GCE, AuNPs/GCE, and Co_3O_4-CHIT/AuNPs/GCE, respectively, these peaks were almost the same position but notably the current was facilitated by the Co_3O_4-CHIT/AuNPs/GCE which make electron transfer easier with the large surface area resulting in a current higher than the bare GCE, Co_3O_4-CHIT/GCE, AuNPs/GCE for 1.79, 2.03, and 1.47 times, respectively.

Optimization of the Co_3O_4-CHIT/AuNPs/GCE using amperometry

The applied potential of the amperometric technique has a very crucial effect on the oxidation current of UA at the Co_3O_4-CHIT/AuNPs/GCE. It was the first variable parameter to be tested from +0.45 to +0.75 V by spiking UA to the final concentration of 0.15 mM in stirred 0.1 M PBS. Figure 2A displays the current obtained versus the applied potential. The current response increased from +0.45 to +0.65 V, and after that, it decreased from +0.65 to +0.75 V. This trend was related to the cyclic voltammogram of UA. The highest current was obtained at +0.65 V and was chosen for further study.

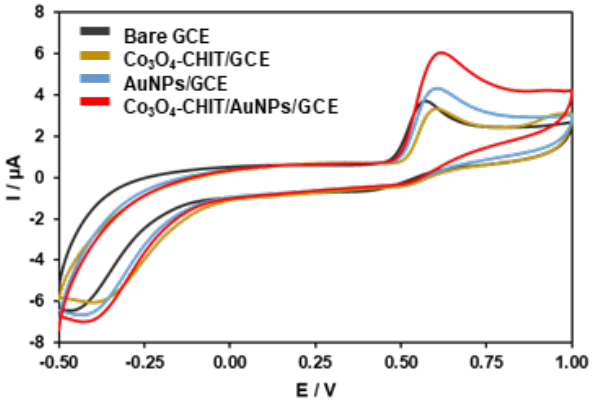

Figure 2 Cyclic voltammograms of bare GCE (black curve), Co_3O_4-CHIT/GCE (brown curve), AuNPs/GCE (blue curve), and Co_3O_4-CHIT/AuNPs/GCE (red curve) of 0.15 mM UA in 0.1 M PBS (pH 7.0) at a scan rate of 50 mV s^{-1}.

Figure 3B shows the obtained currents related to the amount of Co_3O_4 in Co_3O_4-CHIT/AuNPs/GCE. The current steeply increased from 0.0 to 45.0 µg Co_3O_4, reaching its highest at 60.0 µg. It is continuously reduced at 75.0 to 90.0 µg Co_3O_4; the excess thickness causes increased resistance, resulting in lower electron transfer onto the electrode surface [40]. Thus, Co_3O_4 at 60.0 µg was selected for further experiments.

The volume of AuNPs immobilized on the electrode surface varied from 0.0, 10.0, 20.0, 30.0, 40.0, and 50.0 µL in Co_3O_4-CHIT/AuNPs/GCE. The currents were plotted versus the volume of AuNPs in Figure 2C. It was found that 20.0 µL of AuNPs gave the highest signal. The higher excessive AuNPs induced a large barrier to block electron transfer, resulting in lower current at 30.0-50.0 µL.

Figure 2D shows the effect of electrolytes on the signal of 0.15 mM UA at the Co_3O_4-CHIT/AuNPs/GCE. Electrolytes were chosen 0.1 M NaOH, 0.1 M PBS pH 7.0, and acetate buffer pH 5.5 for this study. 0.1 M NaOH and acetate buffer, pH 5.5, can be used as electrolytes, but the currents were lower than in PBS. NaOH shows

DOI: 10.60101/jarst.2024.260199

the lowest obtained current because its pH is more than 10, affecting the precipitation of metal oxide, which resists film conductivity. PBS was chosen for further experiments.

The pH of PBS was varied from pH 6.2 to 7.8 as the electrolyte for UA oxidation at Co_3O_4-CHIT/AuNPs/GCE. The current versus pH of PBS was plotted in Figure 2E. The UA showed the highest oxidation current at pH 7.0, while the current decreased slightly at higher pH 7.4-7.8. The UA oxidation is the preferred basic solution as the product obtains 2 mol of H^+. The elimination of H^+ from the modified electrode surface by reacting with the basic solution, provided the reaction goes forward. Therefore, pH 7.0 can be considered the optimum pH value for detecting UA.

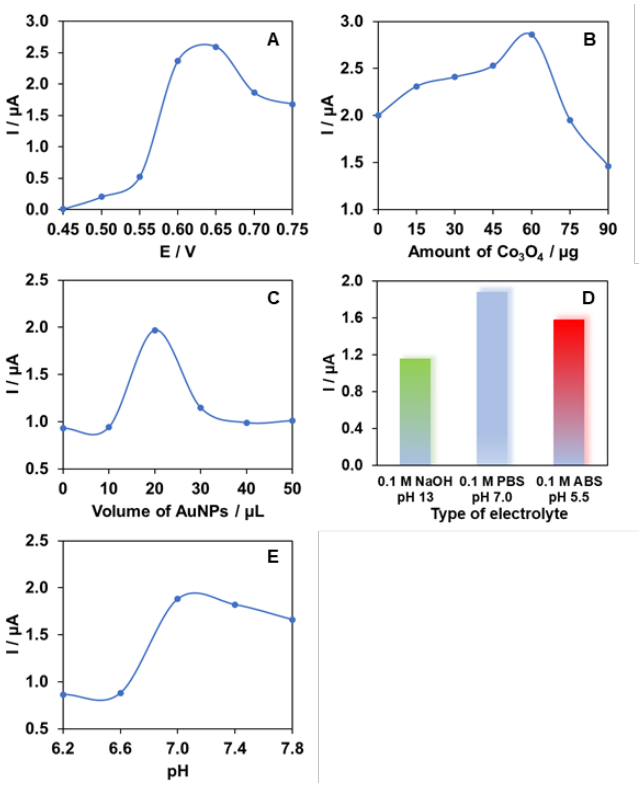

Figure 3 Plot of current response versus variables parameters from the amperometric technique at Co_3O_4-CHIT/AuNPs/GCE; (A) applied potential, (B) amount of Co_3O_4, (C) volume of AuNPs, (D) type of electrolyte, and (E) pH by spiking 0.15 mM.

Linearity

The linearity of UA at Co_3O_4-CHIT/AuNPs/GCE was operated using the obtained conditions by amperometry. Figure 4A shows the successive addition of various concentrations of UA, and the corresponding current versus UA concentration is shown in Figure 4B. There is a linear range from 0.5 – 700 µM ($y = 0.0079x + 0.0049$, $R^2 = 0.9996$). The calculated limit of detection (LOD) (at S/N = 3) was 0.31 µM. Additionally, the limit of quantitation (LOQ) is examined by the equation LOQ= 3.33*LOD, which was found to be 1.03 µM.

Repeatability, reproducibility, interferences, and lifetime

The performance of the Co_3O_4-CHIT/AuNPs/GCE for analyzing UA in terms of repeatability and reproducibility was tested at 0.10 mM UA and 0.15 mM UA, respectively. Figure 5A-red showed the plot of current versus repetition for repeatability assessment by testing five consecutive times at the same Co_3O_4-CHIT/AuNPs/GCE and presenting it in terms of relative standard deviation percentage (%RSD). It showed a value of 2.94 %RSD (n=5). The reproducibility was obtained by operation with the new modifying electrodes at each measurement, and it showed a value of 2.30 %RSD (n=5) in Figure 5A-blue.

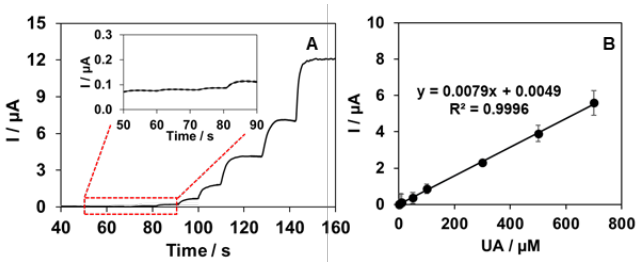

Figure 4 (A) Amperogram of successive addition of UA into 0.1 M PBS pH 7.0 at the Co_3O_4-CHIT/AuNPs/GCE. The inset of A shows zooms in of low UA concentration. (B) Linearity of UA from 0.5 to 700 µM (n=3).

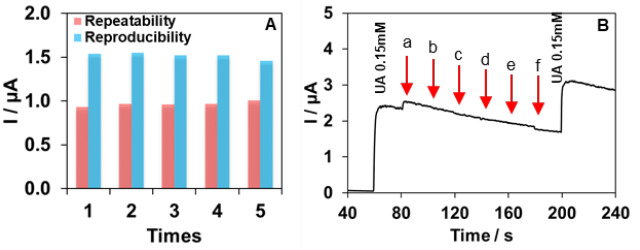

Figure 5 (A) Current response for repeatability (0.10 mM UA) and reproducibility (0.15 mM UA) at Co_3O_4-CHIT/AuNPs/GCE sensor. (B) amperogram of interference effect on the analysis of 0.15 mM UA by spiking of a) 0.01 mM ascorbic acid, b) 0.5 mM urea, c) 0.1 mM caffeine, d) 5.0 mM Cl^-, e) 7.0 mM glucose, and f) 20.0 mM sucrose.

In the study of interference ions of UA, we focused on the ions in blood where UA is present. We select interferences, including ascorbic acid, urea, caffeine, Cl^-, glucose, and sucrose. These compounds were selected because they are commonly derived from dietary intake, are naturally present in the bloodstream, and have oxidation peak potentials close to that of UA, which may potentially interfere with the assay. We found that 0.01 mM ascorbic acid, 0.5 mM urea, 0.1 mM caffeine, 5.0 mM Cl^-, 7.0 mM glucose, and 20.0 mM sucrose did not influence the analyzed UA. Figure 5B shows the amperogram of spiking 0.15

DOI: 10.60101/jarst.2024.260199

mM UA and interfering ions. This evidence proves that the Co_3O_4-CHIT/AuNPs/GCE can be used for UA in the presence of interfering ions. The selectivity of this sensor using metal nanoparticles (Co_3O_4 and AuNPs) reduces interferences contributing to the current signal [34]. Our work agrees that metal nanoparticles enhance selectivity by favoring UA oxidation while suppressing glucose and urea oxidation, as reported by the previous work [36, 41]. Similarly, caffeine does not interfere with this sensor as their oxidation occurs at significantly higher potentials (above +1.2 V vs. Ag/AgCl) [42]. The Cl^- is electrochemically stable and does not oxidize at +0.65 V, ensuring selectivity [43-45]. The direct electrochemical oxidation of sucrose is possible under specific conditions [46]. However, the molecular complexity of sucrose poses challenges, preventing any significant interference. Ascorbic acid is primarily oxidized at lower potentials and is often fully consumed before reaching the applied potential of +0.65 V of Co_3O_4-CHIT/AuNPs/GCE, minimizing its impact.

For the lifetime usage of the modified electrode, we examined continuous operation and found it could be used for 29 cycles in a single preparation. (data do not show). The current from the first five experiments is still higher than 95% compared to the first one.

Determination of uric acid in blood samples

Using the standard addition method, the Co_3O_4-CHIT/AuNPs/GCE sensor was applied to detect UA in blood samples. UA was detectable in all four samples. These samples were then spiked with known concentrations of UA and subsequently re-analyzed. The percentage of recovery was calculated and shown in Table 1. This sensor showed high accuracy, with recovery percentages ranging from 96.76% to 104.92%. The performance of the Co_3O_4-CHIT/AuNPs/GCE sensor for UA was compared to previously reported methods, as summarized in Table 2.

Table 1 Determination of UA concentrations in blood samples.

Samples	UA in sample / µM	Spiked UA / µM	Found UA / µM	%Recovery
1	7.1	200.00	200.6	96.76
2	10.6	200.0	214.5	101.96
3	1.4	200.0	207.6	103.06
4	4.7	200.0	214.5	104.92

Table 2 Comparison of UA sensors by electrochemical approach.

Electrodes	Technique	Linear (µM)	LOD (µM)	Ref.
ITO-ERGO/ZnO	Amperometry	1–400	0.45	[47]
Co_3O_4 porous NSs/GCE	DPV	0-800	12.0	[34]
Co_3O_4-MWCNTs/GCE	CV	100-3,000	5.0	[36]
Co_3O_4 nanostructures/GCE	CV	500-3,500	100.0	[48]
Nafion/Uricase/ZnO/Au	Amperometry	100-590	25.6	[49]
Uricase/AuNPs/MWCNTs/Au	Amperometry	10-800	10.0	[50]
Co_3O_4-CHIT/AuNPs/GCE	Amperometry	0.5-700	0.31	This work

ITO, indium tin oxide electrode; ERGO, electrochemically reduced graphene oxide; ZnO, zine oxide; GCE, glassy carbon electrode; Co_3O_4, tricobalt tetroxide; NSs, nanosheets; DPV, differential pulse voltammetry; MWCNTs, multi-walled carbon nanotubes; CV, cyclic voltammetry; Au, gold electrode; AuNPs, gold nanoparticles.

CONCLUSIONS

In summary, a highly effective UA sensor was successfully developed using Co_3O_4-CHIT/AuNPs modified on a glassy carbon electrode GCE. Incorporating Co_3O_4, CHIT, and AuNPs significantly enhanced the sensor's response to UA due to their synergistic properties. The sensor demonstrated excellent analytical performance, with a wide detection range of 0.5 to 700 µM and a low detection limit of 0.31 µM. Moreover, the sensor exhibited outstanding stability, ease of operation, and strong selectivity. Its long operational lifetime and high accuracy are reflected in a percentage recovery of 96.76% to 104.92%. These results suggest that the Co_3O_4-CHIT/AuNPs/GCE sensor is a promising tool for UA detection in biological samples.

ACKNOWLEDGEMENT

This research project is supported by the National Research Council of Thailand (NRCT) : (Contact No. N41A650115). The author appreciates and acknowledges the Sansai Hospital for providing real blood samples for blinding tests.

DOI: 10.60101/jarst.2024.260199

REFERENCES

1. Maiuolo J, Oppedisano F, Gratteri S, Muscoli C, Mollace V. Regulation of uric acid metabolism and excretion. Int J Cardiol. 2016;213:8-14.
2. Xu L, Li C, Wan T, Sun X, Lin X, Yan D, et al. Targeting uric acid: a promising intervention against oxidative stress and neuroinflammation in neurodegenerative diseases. Cell Commun Signal. 2025;23(1):4.
3. Swinson D, Snaith J, Buckberry J, Brickley M. High performance liquid chromatography (HPLC) in the investigation of gout in palaeopathology. Int J Osteoarchaeol. 2010;20(2):135-43.
4. Li Q, Qiu Y, Han W, Zheng Y, Wang X, Xiao D, et al. Determination of uric acid in biological samples by high performance liquid chromatography-electrospray ionization-tandem mass spectrometry and study on pathogenesis of pulmonary arterial hypertension in pulmonary artery endothelium cells. RSC Adv. 2018;8(45):25808-14.
5. Rocha DL, Rocha FR. A flow-based procedure with solenoid micro-pumps for the spectrophotometric determination of uric acid in urine. Microchem J. 2010;94(1):53-9.
6. Yan Q, Zhi N, Yang L, Xu G, Feng Q, Zhang Q, et al. A highly sensitive uric acid electrochemical biosensor based on a nano-cube cuprous oxide/ferrocene/uricase modified glassy carbon electrode. Sci Rep. 2020;10(1):10607.
7. Zhang Y, Lei W, Xu Y, Xia X, Hao Q. Simultaneous detection of dopamine and uric acid using a poly (l-lysine)/graphene oxide modified electrode. Nanomater. 2016;6(10):178.
8. Jin D, Seo MH, Huy BT, Pham QT, Conte ML, Thangadurai D, et al. Quantitative determination of uric acid using CdTe nanoparticles as fluorescence probes. Biosens Bioelectron. 2016;77:359-65.
9. Hashem SG, Elsaady MM, Afify HG, Omer WE, Youssef AO, El-Kemary M, et al. Determination of uric acid in serum using an optical sensor based on binuclear Pd(II) 2-pyrazinecarboxamide-bipyridine doped in a sol gel matrix. Talanta. 2019;199:89-96.
10. Nishan U, Ullah W, Muhammad N, Asad M, Afridi S, Khan M, et al. Development of a nonenzymatic colorimetric sensor for the detection of uric acid based on ionic liquid-mediated nickel nanostructures. ACS Omega. 2022;7(30):26983-91.
11. Akbari S, Jahani S, Foroughi MM, Hassani Nadiki H. Simultaneous determination of methadone and morphine at a modified electrode with 3D β-MnO_2 nanoflowers: application for pharmaceutical sample analysis. RSC Adv. 2020;10(63):38532-45.
12. Noroozifar M, Khorasani-Motlagh M, Hassani Nadiki H, Saeed Hadavi M, Mehdi Foroughi M. Modified fluorine-doped tin oxide electrode with inorganic ruthenium red dye-multiwalled carbon nanotubes for simultaneous determination of a dopamine, uric acid, and tryptophan. Sens Actuators, B. 2014;204:333-41.
13. Randviir EP, Banks CE. A review of electrochemical impedance spectroscopy for bioanalytical sensors. Anal Methods. 2022;14(45):4602-24.
14. Foroughi MM, Jahani S, Rashidi S, Tayari O, Moradalizadeh M. The development of electrochemical DNA biosensor based on woolen ball-shaped La^{3+}/TiO_2 nanostructure coating: nanomolar detection of vinorelbine. Mater Chem Phys. 2024;315:128893.
15. Hajmalek S, Jahani S, Foroughi MM. Simultaneous voltammetric determination of tramadol and paracetamol exploiting glassy carbon electrode modified with FeNi3 nanoalloy in biological and pharmaceutical media. Chemistry Select. 2021;6(33): 8797-808.
16. Omar MN, Salleh AB, Lim HN, Ahmad Tajudin A. Electrochemical detection of uric acid via uricase-immobilized graphene oxide. Anal Biochem. 2016; 509:135-41.
17. Jirakunakorn R, Khumngern S, Choosang J, Thavarungkul P, Kanatharana P, Numnuam A. Uric acid enzyme biosensor based on a screen-printed electrode coated with Prussian blue and modified with chitosan-graphene composite cryogel. Microchem J. 2020;154:104624.
18. Chaiya N, Tapala W, Kunthadee P, Ladrodphan N, Tangkuaram T, Puntharod R. Hydrothermal synthesis of tricobalt tetroxide and characterization. PSRU J Sci Technol. 2023;8(3):20-9.
19. Dongsheng Z, Youlan Y, Yaping D, Rong F. An amperometric l-tryptophan sensor platform based on electrospun tricobalt tetroxide nanoparticles decorated carbon nanofibers. Sens Actuators, B. 2017;241:601-6.
20. Zhou T, Zhang T, Deng J, Zhang R, Lou Z, Wang L. P-type Co_3O_4 nanomaterials-based gas sensor: preparation and acetone sensing performance. Sens Actuators, B. 2017;242:369-77.
21. Vladimirova S, Krivetskiy V, Rumyantseva M, Gaskov A, Mordvinova N, Lebedev O, et al. Co_3O_4 as p-yype material for CO sensing in humid air. Sensors. 2017;17(10).
22. Soomro RA, Nafady A, Ibupoto ZH, Sirajuddin, Sherazi STH, Willander M, Abro MI. Development of sensitive non-enzymatic glucose sensor using

DOI: 10.60101/jarst.2024.260199

complex nanostructures of cobalt oxide. Mater Sci Semicond Process. 2015;34:373-81.

23. Zallouz S, Réty B, Vidal L, Le Meins JM, Matei Ghimbeu C. Co_3O_4 nanoparticles embedded in mesoporous carbon for supercapacitor applications. ACS Appl Nano Mater. 2021;4(5):5022-37.
24. Hu Z, Hao L, Quan F, Guo R. Recent developments of Co_3O_4-based materials as catalysts for the oxygen evolution reaction. Catal Sci Technol. 2022;12(2):436-61.
25. Yeh YC, Creran B, Rotello VM. Gold nanoparticles: preparation, properties, and applications in bionanotechnology. Nanoscale. 2012;4(6):1871-80.
26. Rajendran G, Rajamuthuramalingam T, Michael Immanuel Jesse D, Kathiravan K. Synthesis and characterization of biocompatible acetaminophen stabilized gold nanoparticles. Mater Res Express. 2019;6(9):095043.
27. Niżnik Ł, Noga M, Kobylarz D, Frydrych A, Krośniak A, Kapka-Skrzypczak L, et al. Gold nanoparticles (AuNPs)-toxicity, safety and green synthesis: a critical review. Int J Mol Sci. 2024;25(7):4057.
28. Ismail S, Yusof NA, Abdullah J, Abd Rahman SF. Development of electrochemical sensor based on silica/gold nanoparticles modified electrode for detection of arsenite. IEEE Sens J. 2020;20:3406-14.
29. Yang Q, Zhang X, Kumar S, Singh R, Zhang B, Bai C, et al. Development of glucose aensor using gold nanoparticles and glucose-oxidase functionalized tapered fiber structure. Plasmonics. 2020;15(3):841-8.
30. Bocchetta P, Othman A, Gupta M, Andriani G, Martin P, Kumar Y, et al. Chitosan in electrochemical (bio)sensors: nanostructuring and methods of synthesis. Eur Polym J. 2024;213:113092.
31. Bounegru AV, Bounegru I. Chitosan-based electrochemical sensors for pharmaceuticals and clinical applications. Polym. 2023;15(17):3539.
32. Chmayssem A, Shalayel I, Marinesco S, Zebda A. Investigation of GOx stability in a chitosan aatrix: applications for enzymatic electrodes. Sensors. 2023;23(1):465.
33. Chachuli SAM, Muhammad Azmi NA, Shamsudin NH, Coban O, Aziz SAC. Impact of chitosan as a binder in graphene gas sensor for volatile organic compound detection. Chemistry Select. 2025;10(4):e202405111.
34. Masrat S, Nagal V, Khan M, Moid I, Alam S, Bhat KS, et al. Electrochemical ultrasensitive sensing of uric acid on non-enzymatic porous cobalt oxide nanosheets-based sensor. Biosensors. 2022;12(12):1140.
35. Tangkuaram T, Ponchio C, Kangkasomboon T, Katikawong P, Veerasai W. Design and development of a highly stable hydrogen peroxide biosensor on screen printed carbon electrode based on horseradish peroxidase bound with gold nanoparticles in the matrix of chitosan. Biosens Bioelectron. 2007;22(9-10):2071-8.
36. Lal R, Bhatia BL, Tahira A, Shaikh SF, Alsalme AM, Al-Othman AA, et al. Synthesis of composite material of cobalt oxide (Co_3O_4) with hydroxide functionalized multi-walled carbon nanotubes (MWCNTs) for electrochemical determination of uric acid. J Mater Sci Mater Electron. 2021;32(15):20047-57.
37. Papafilippou L, Claxton A, Dark P, Kostarelos K, Hadjidemetriou M. Nanotools for sepsis diagnosis and treatment. Adv Healthc Mater. 2020;10:2001378.
38. Subara D, Jaswir I. Gold nanoparticles: synthesis and application for halal authentication in meat and meat products. Int J Adv Sci Eng Inf Technol. 2018;8:1633-41.
39. Krishnamoorthy K, Sudha V, Senthil Kumar SM, Thangamuthu R. Simultaneous determination of dopamine and uric acid using copper oxide nano-rice modified electrode. J Alloys Compd. 2018;748:338-47.
40. Tang T, Zhou M, Lv J, Cheng H, Wang H, Qin D, et al. Sensitive and selective electrochemical determination of uric acid in urine based on ultrasmall iron oxide nanoparticles decorated urchin-like nitrogen-doped carbon. Colloids Surf B. 2022;216:112538.
41. Turkkan G, Bas SZ, Atacan K, Ozmen M. An electrochemical sensor based on a Co_3O_4–ERGO nanocomposite modified screen-printed electrode for detection of uric acid in artificial saliva. Anal Methods. 2022;14(1):67-75.
42. Mersal GAM. Experimental and computational studies on the electrochemical oxidation of caffeine at pseudo carbon paste electrode and its voltammetric determination in different real samples. Food Anal Methods. 2012;5(3):520-9.
43. Du J, Chen Z, Chen C, Meyer TJ. A half-reaction alternative to water oxidation: chloride oxidation to chlorine catalyzed by silver ion. J Am Chem Soc. 2015;137(9):3193-6.
44. Niu X, Li X, Pan J, He Y, Qiu F, Yan Y. Recent advances in non-enzymatic electrochemical glucose sensors based on non-precious transition metal materials: opportunities and challenges. RSC Adv. 2016;6(88):84893-905.

DOI: 10.60101/jarst.2024.260199

JOURNAL OF APPLIED RESEARCH ON SCIENCE AND TECHNOLOGY

45. Hassan MH, Vyas C, Grieve B, Bartolo P. Recent advances in enzymatic and non-enzymatic electrochemical glucose sensing. Sensors. 2021;21 (14):4672.

46. Asghar N, Mustafa G, Jabeen N, Dawood A, Rida, Jabeen Z, Malik QH, et al. Fabrication of efficient and non-enzymatic electrochemical sensors for the detection of sucrose. Sensors. 2023;23(4):2008.

47. Eryiğit M, Urhan BK, Doğan HÖ, Özer TÖ, Demir Ü. ZnO nanosheets-decorated ERGO layers: an efficient electrochemical sensor for non-enzymatic uric acid detection. IEEE Sens J. 2022;22(6):5555-61.

48. Chang AS, Tahira A, Chang F, Memon NN, Nafady A, Kasry A, et al. Silky Co_3O_4 nanostructures for the selective and sensitive enzyme free sensing of uric acid. RSC Adv. 2021;11(9):5156-62.

49. Zhao Y, Yan X, Kang Z, Pei L, Fang X, Lei Y, et al. Highly sensitive uric acid biosensor based on individual zinc oxide micro/nanowires. Microchim Acta. 2013;180.

50. Chauhan N, Pundir C. An amperometric uric acid biosensor based on multiwalled carbon nanotube-gold nanoparticle composite. Anal Biochem. 2011; 413:97-103.

DOI: 10.60101/jarst.2024.260199